Supplementary Information (SI) for Reaction Chemistry & Engineering.
This journal is © The Royal Society of Chemistry 2025

**Supporting information**

# Enhanced Thermostability of $C_2$-Symmetrical Bis(imino)pyridine–Iron Precatalysts for Ethylene Polymerization via a Hybrid Steric Strategy

Shuangshuang Liu,[a,b,c] Qiuyu Li,[b,c] Qaiser Mahmood,[b,*] Zhixin Yu,[a,*] Yizhou Wang,[d] Ran Zhang,[b,c] Geng Ren,[d] Wen-Hua Sun[a,b,d,*]

[a] School of Pharmaceutical Sciences, Changchun University of Chinese Medicine, Changchun 130117, China.
[b] Chemistry and Chemical Engineering Guangdong Laboratory, Shantou, 515031, China
[c] AstaTech Biopharmaceutical Corporation, Chengdu 610095, China
[d] Key Laboratory of Engineering Plastics, Beijing National Laboratory for Molecular Sciences, Institute of Chemistry, Chinese Academy of Sciences, Beijing 100190, China.
Corresponding authors Email: qaiser@ccelab.com.cn (Q. M); yuzx01@ccucm.edu.cn (Z. Y); whsun@iccas.ac.cn (W.-H. S.)

## Contents

## 1. General conditions and materials

All reactions involving air and moisture sensitivity are carried out under nitrogen conditions (nitrogen purity ≥ 99%), distilled to remove water and oxygen from toluene, and dry toluene is used for ethylene polymerization reaction. The diphenylmethanol, zinc chloride, 2,6-diacetylpyridine, and 2,6-diisopropylaniline used in the experiment were all purchased from McLean Company with a purity of ≥ 98%, while toluene was purchased from Xihua Company, purity ≥ 99.5%, and water ≤ 0.03%. Before use, water was distilled off with sodium, and high-purity ethylene was obtained from Guangdong Jieyang Petrochemical Company. Methylaluminoxane (MAO, 1.67 M in toluene) and modified methylaluminoxane (MMAO, 1.93 M in heptane) were purchased from Anhui Botai Electronic Materials Co., Ltd. The $^{1}H$ and $^{13}C$ NMR spectra of organic compounds were measured using a Bruker AVANCE III 600WB spectrometer at 600 MHz, with 1024 and 16 scans performed, respectively. Working conditions for $^{1}H$ and $^{13}C$ spectra: spectral width of 15.0 kHz; Collection time 2.1845 seconds; Relaxation delay of 2.0 seconds. The chemical shift is measured in ppm for $^{1}H$ and $^{13}C$ NMR spectra, and relative to TMS as an internal standard. Elemental analysis tests were performed on the Flash EA 1112 microanalyzer. FTIR infrared spectroscopy was performed using a PerkinElmer system 2000 FTIR infrared spectrometer. After mixing and grinding the sample with evenly ground potassium bromide particles and maintain the concentration of the sample in potassium bromide within the range of 0.2% to 1%. The frequency range is usually measured within the range of 4000-400 $cm^{-1}$, and data processing is performed using OMNIC software. At 150 ℃, the molecular weight ($M_w$) and molecular weight distribution (PDI) of polyethylene were determined using PL-GPC220 instrument with 1,2,4-trichlorobenzene (TCB) as the solvent. The flow rate of TCB is maintained at 1.00 mL/min, with an injection volume of 200.0 μL and a stable column length of 650 mm. The specification of the column used is 2 × PLgel MIXED-B 10 μm 300 × 7.5 mm. The sample concentration is maintained at 0.1 mg/mL. The melting temperature of polyethylene were mearured using a PerkinElmer TA-Q2000 DSC analyzer under a nitrogen atmosphere. During this process, a sample of approximately 4.0-6.0

milligrams was heated to 150 ℃ at a heating rate of 20 ℃ $min^{-1}$, and stored at 150 ℃ for 5 minutes to remove thermal history. Then, it was cooled at a rate of 20 ℃ $min^{-1}$ to 25 ℃. The peak value obtained from the second scan measurement was the melting point of polyethylene. Using deuterated tetrachloroethane as the solvent and TMS as the internal standard, peak integration was performed using the area removal method. The $^{1}H$ and $^{13}C$ nuclear magnetic spectra of polyethylene were recorded using a Bruker DMX 300 MHz instrument at 110 ℃. Operating conditions for $^{1}H$ spectrum: spectral width of 15 kHz; Collection time 2.1889 seconds; Relaxation delay of 2.0 seconds. Operating conditions for $^{13}C$ spectrum: spectral frequency of 125.70 MHz; Pulse width 10.0 ms; Spectral width 21.3675 kHz; Collection time 0.7668 seconds; Relaxation delay of 5.0 seconds; Scan 2048 times. The chemical shift value (δ) is expressed in parts per million (ppm).

**2. General method of ethylene polymerization**

The polymerization process at 1MPa ethylene pressure was conducted in a 250 mL stainless steel autoclave equipped with an ethylene pressure control system, a mechanical stirrer, and a temperature controller. Initially, the autoclave was dried, then purged twice with nitrogen and once with ethylene under reduced pressure to ensure an inert environment. Then, the complex (2.0 μmol) was dissolved in 30 mL of toluene and injected into the autoclave at the required reaction temperature. An additional 30 mL of toluene was added for washing purposes. Next, the appropriate amount of co-catalyst (MAO, or MMAO) and more toluene were added successively to reach a total volume of 100 mL. The autoclave was immediately pressurized with 1 MPa of ethylene, and stirring was initiated. After the desired reaction time, the ethylene pressure was released, and the reaction was quenched by adding 10% hydrochloric acid in ethanol. The resulting polymer was collected, washed with ethanol, dried under reduced pressure at room temperature, and then weighed.

**3. X-ray crystallographic studies**

The single-crystal X-ray diffraction analysis of $\mathbf{Fe^{F}}$ and $\mathbf{Fe^{Bh}}$ complexes were conducted using a Rigaku Sealed Tube CCD (Saturn 724+) diffractometer, Japan. The diffractometer employed graphite-monochromated Cu-Kα radiation with a wavelength (λ) of 1.54184 Å. The measurements were performed at a temperature of 170 (±10) K. The cell parameters were determined by globally refining the positions

of all collected reflections. The intensities obtained from the X-ray diffraction analysis were corrected for Lorentz and polymerization effects; an empirical absorption correction was carried out as well. The structures of complexes **Fe$^{F}$** and **Fe$^{Bh}$** were identified via direct methods and further refined via full-matrix least squares fitting on F2. The non-hydrogen atoms in each complex were refined anisotropically. The positions of all hydrogen atoms were determined based on calculated positions. The structural solution and refinement for each complex were carried out using SHELXT (Sheldrick) software.[1] The crystal data and processing parameters for **Fe$^{F}$** and **Fe$^{Bh}$** are presented in Table S1.

**Table S1. Crystal data and structure refinement for Fe$^{F}$ and Fe$^{Bh}$**

| | **Fe$^{F}$** | **Fe$^{Bh}$** |
|---|---|---|
| Empirical formula | $C_{73}H_{57}Cl_2F_2FeN_3$ | $C_{99}H_{79}Cl_2FeN_3$ |
| Formula weight | 1140.97 | 1437.41 |
| Temperature/K | 170.00(10) | 170.00(10) |
| Crystal system | monoclinic | monoclinic |
| Space group | $P2_1/c$ | $P2_1/c$ |
| a/Å | 13.1930(3) | 15.8137(3) |
| b/Å | 18.6712(4) | 31.7044(8) |
| c/Å | 26.3650(6) | 18.3282(5) |
| α/° | 90 | 90 |
| β/° | 92.422(2) | 108.752(3) |
| γ/° | 90 | 90 |
| Volume/Å$^3$ | 6488.6(2) | 8701.3(4) |
| Z | 4 | 4 |
| $\rho_{calc}$g/cm$^3$ | 1.293 | 1.208 |
| μ/mm$^{-1}$ | 3.044 | 3.351 |
| F(000) | 2660.0 | 3299.0 |
| Crystal size/mm$^3$ | 0.22 × 0.18 × 0.12 | 0.2 × 0.15 × 0.08 |
| Radiation | Cu Kα (λ = 1.54184) | Cu Kα (λ = 1.54184) |
| 2Θ range for data collection/° | 5.802 to 152.552 | 6.528 to 133.182 |
| Index ranges | -16 ≤ h ≤ 15, -22 ≤ k ≤ 22, -33 ≤ l ≤ 31 | -18 ≤ h ≤ 15, -37 ≤ k ≤ 37, -21 ≤ l ≤ 21 |
| Reflections collected | 46900 | 59612 |
| Independent reflections | 13043 [$R_{int}$ = 0.0719, $R_{sigma}$ = 0.0571] | 15003 [$R_{int}$ = 0.0807, $R_{sigma}$ = 0.0527] |
| Data/restraints/parameters | 13043/0/733 | 15003/865/992 |
| Goodness-of-fit on F$^2$ | 1.057 | 1.030 |
| Final R indexes [I>=2σ (I)] | $R_1$ = 0.0568, $wR_2$ = 0.1540 | $R_1$ = 0.1077, $wR_2$ = 0.2794 |

| | | |
|---|---|---|
| Final R indexes [all data] | $R_1 = 0.0784$, $wR_2 = 0.1659$ | $R_1 = 0.1273$, $wR_2 = 0.2968$ |
| Largest diff. peak/hole / e Å$^{-3}$ | 0.49/-0.40 | 1.42/-0.70 |

## 4. GPC curves of obtained polyethylene using different catalysts at different conditions

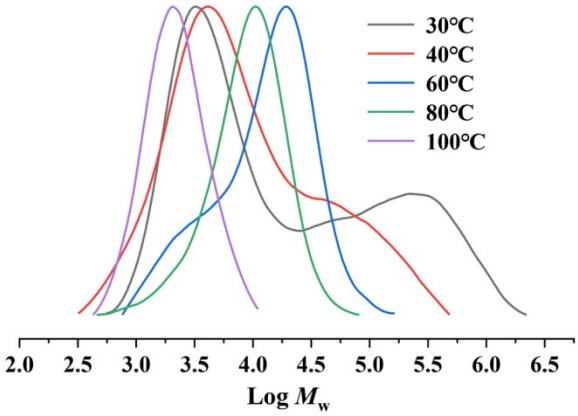


**Figure S1.** GPC curves of polyethylene obtained using $Fe^{Me}$ as precatalyst and MMAO as cocatalyst at different temperatures (Table 3, entries 1-5).

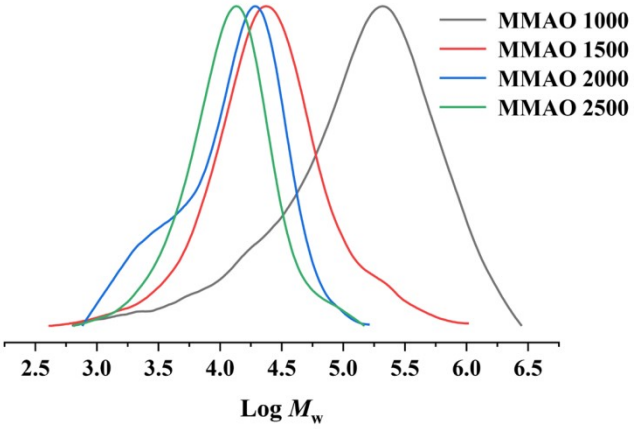


**Figure S2.** GPC curves of polyethylene obtained using $Fe^{Me}$ as precatalyst and MMAO as cocatalyst at different Al/Fe ratios (Table 3, entries 3,6-8).

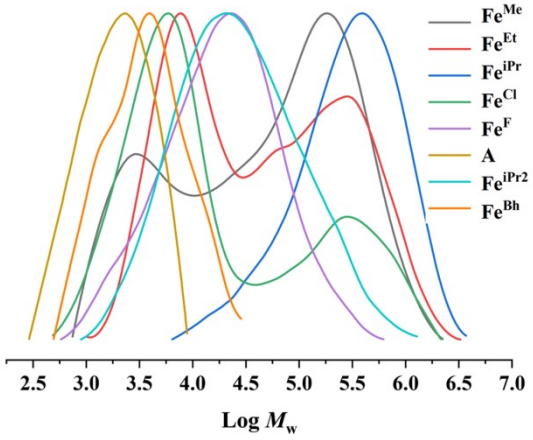


**Figure S3.** GPC curves of polyethylene obtained using different precatalysts and MAO as

cocatalyst at Al/Fe ratios (Table 4, entries 1-8).

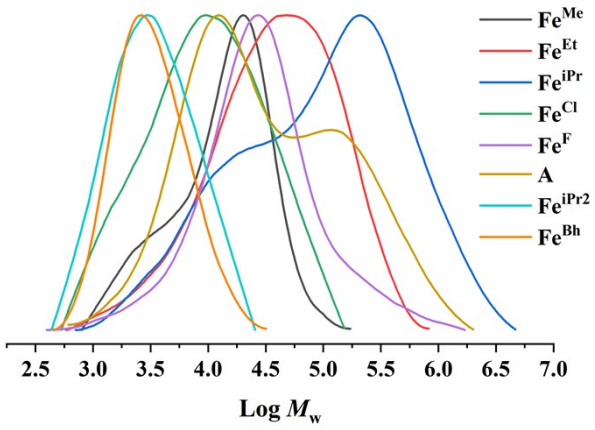


**Figure S4.** GPC curves of polyethylene obtained using different precatalysts and MMAO as cocatalyst at Al/Fe ratios (Table 4, entries 9-16).

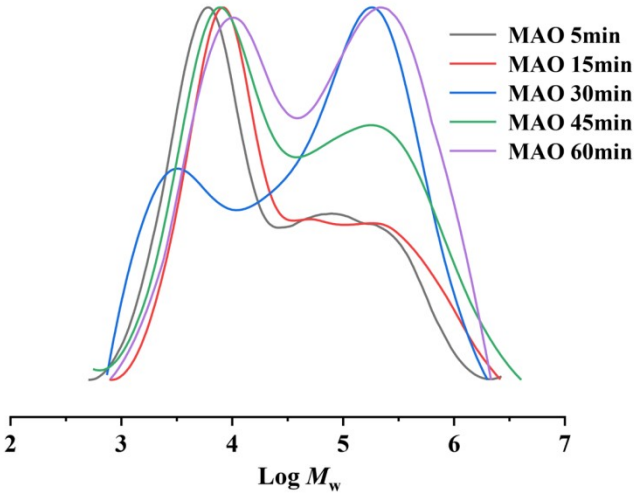


**Figure S5.** GPC curves of polyethylene obtained using $Fe^{Me}$ as precatalyst and MAO as cocatalyst at different reaction time (Table 5).

## 5. DSC thermograms of polyethylene obtained at different temepratures and using different catalysts

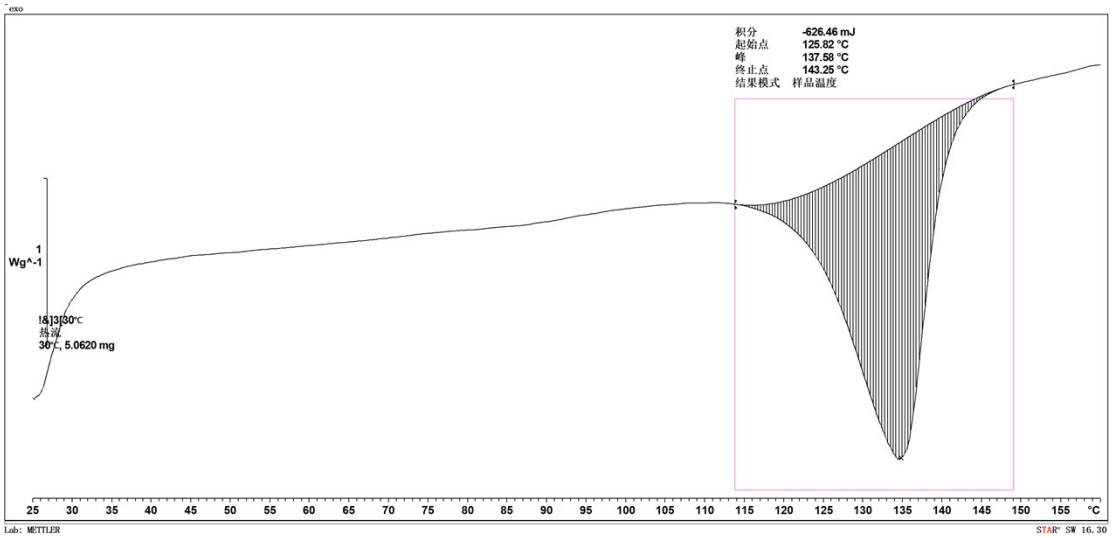


**Figure S6.** DSC thermogram of obtained polyethylene using $Fe^{Me}$ as precatalyst and MAO as cocatalyst at 30 ℃ (Table 2, entry 1).

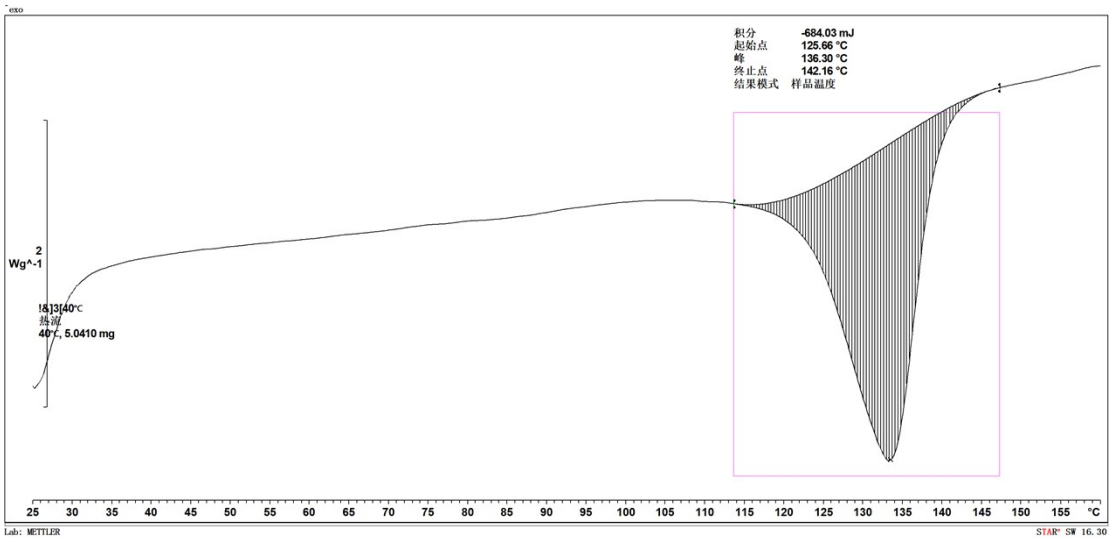


**Figure S7.** DSC thermogram of obtained polyethylene using $Fe^{Me}$ as precatalyst and MAO as cocatalyst at 40 ℃ (Table 2, entry 2).

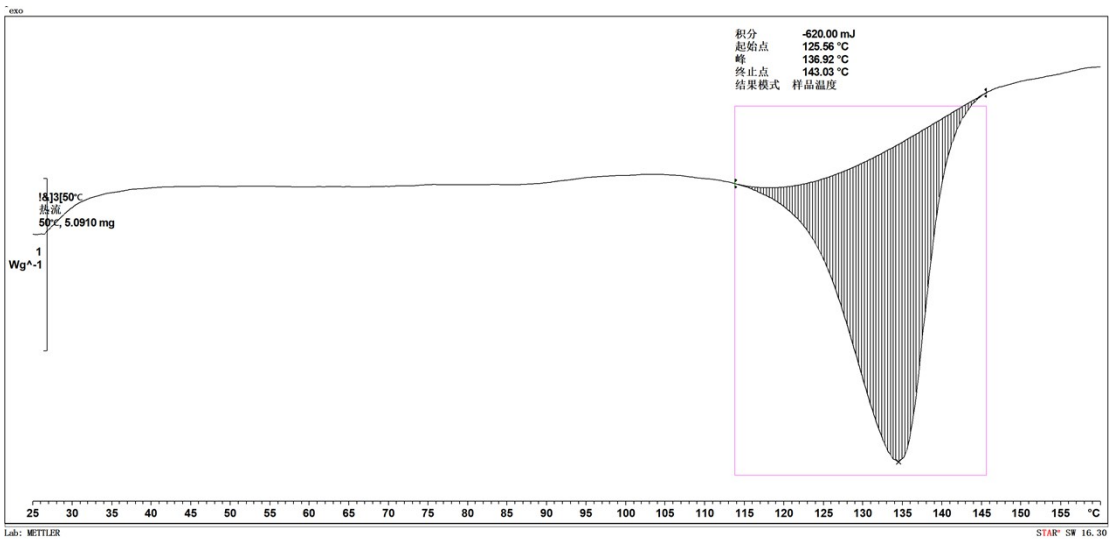


**Figure S8.** DSC thermogram of obtained polyethylene using $Fe^{Me}$ as precatalyst and MAO as cocatalyst at 50 °C (Table 2, entry 3).

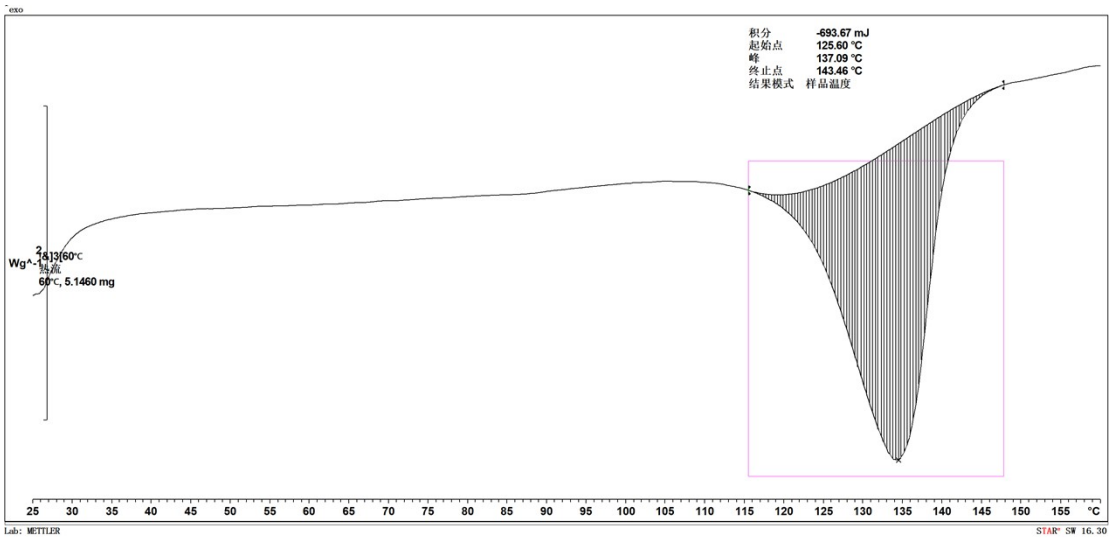


**Figure S9.** DSC thermogram of obtained polyethylene using $Fe^{Me}$ as precatalyst and MAO as cocatalyst at 60 °C (Table 2, entry 4).

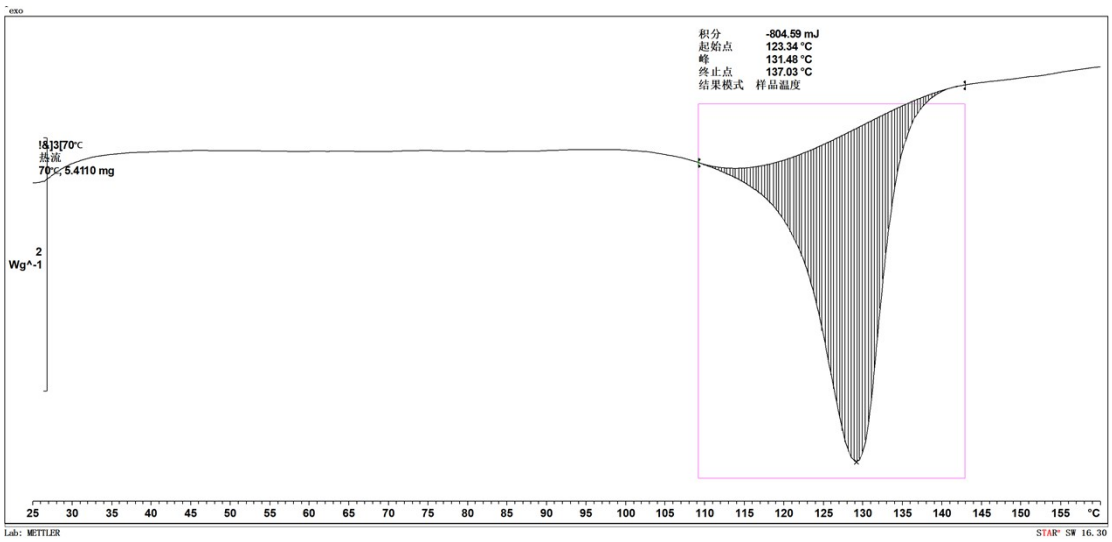


**Figure S10.** DSC thermogram of obtained polyethylene using $Fe^{Me}$ as precatalyst and MAO as cocatalyst at 70 ℃ (Table 2, entry 5).

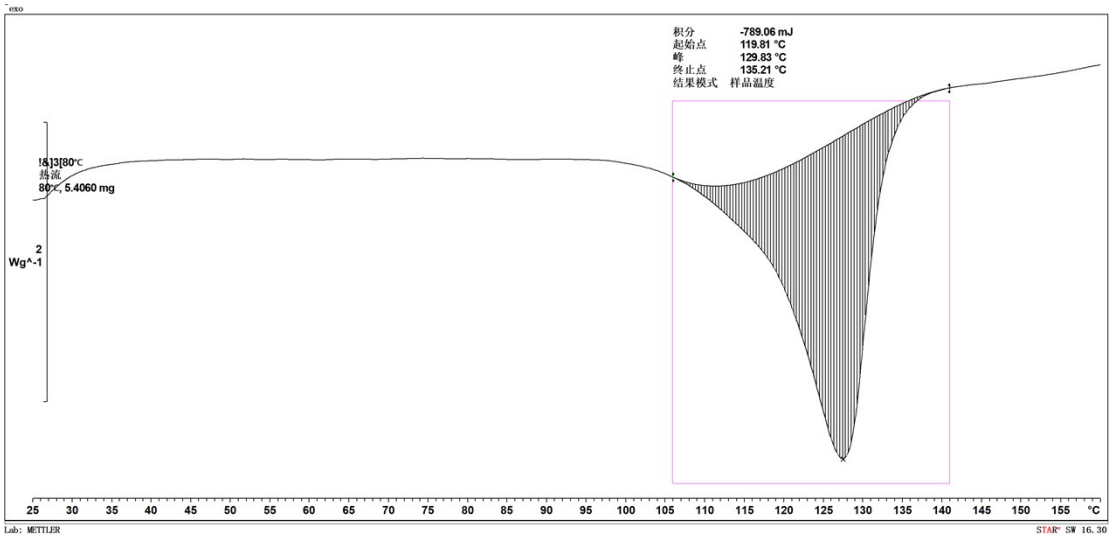


**Figure S11.** DSC thermogram of obtained polyethylene using $Fe^{Me}$ as precatalyst and MAO as cocatalyst at 80 ℃ (Table 2, entry 6).

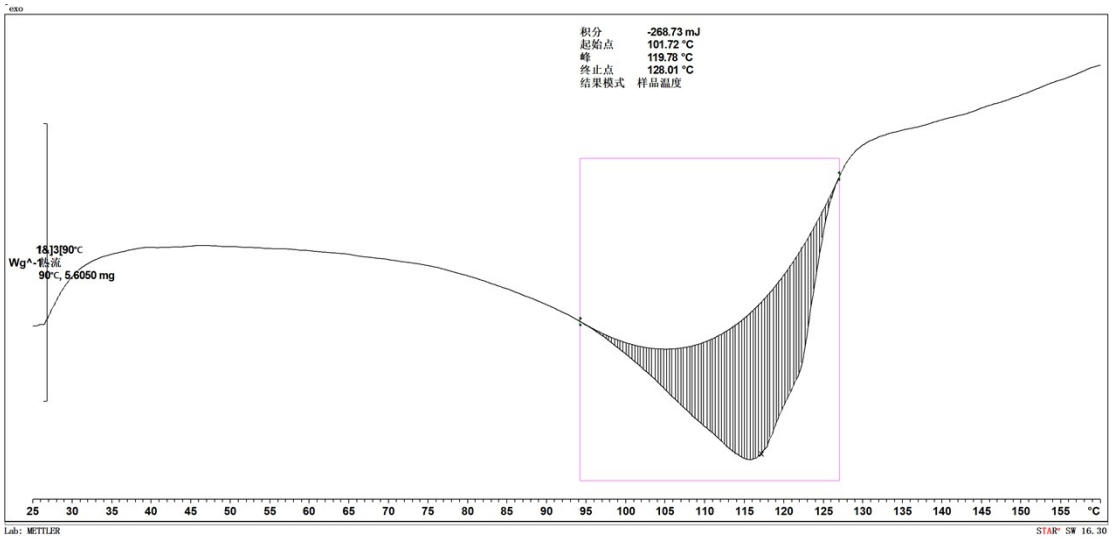


**Figure S12.** DSC thermogram of obtained polyethylene using $Fe^{Me}$ as precatalyst and MAO as cocatalyst at 90 °C (Table 2, entry 7).

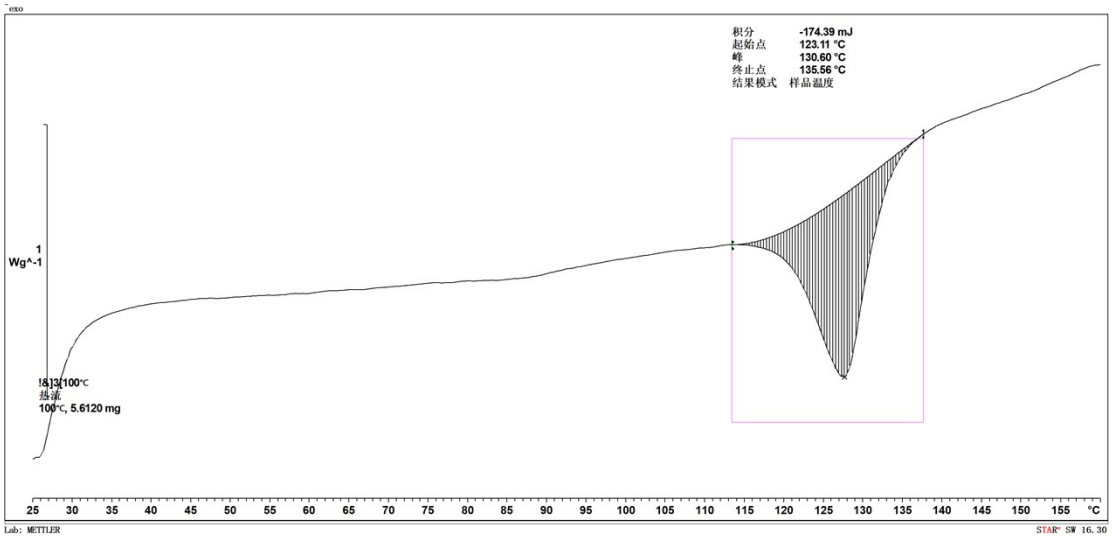


**Figure S13.** DSC thermogram of obtained polyethylene using $Fe^{Me}$ as precatalyst and MAO as cocatalyst at 100 °C (Table 2, entry 8).

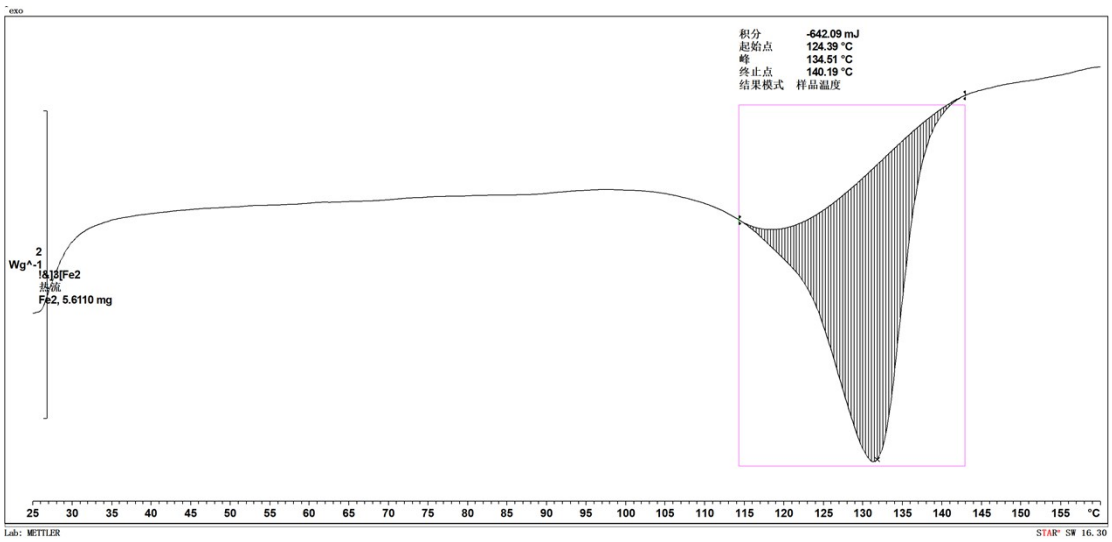


**Figure S14.** DSC thermogram of obtained polyethylene using $Fe^{Et}$ as precatalyst and MAO as cocatalyst at 60 ℃ (Table 4, entry 4).

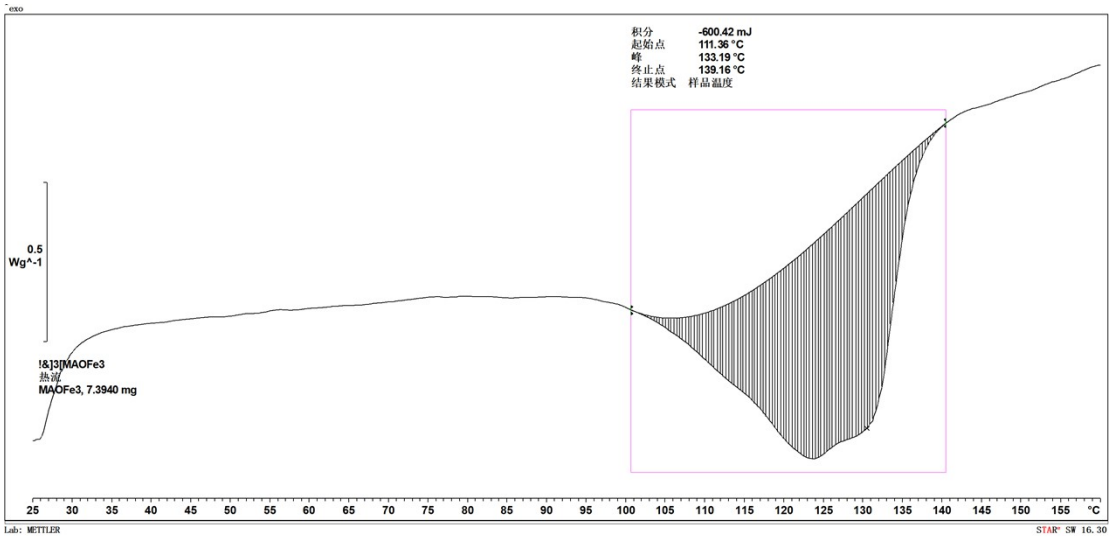


**Figure S15.** DSC thermogram of obtained polyethylene using $Fe^{iPr}$ as precatalyst and MAO as cocatalyst at 60 ℃ (Table 4, entry 5).

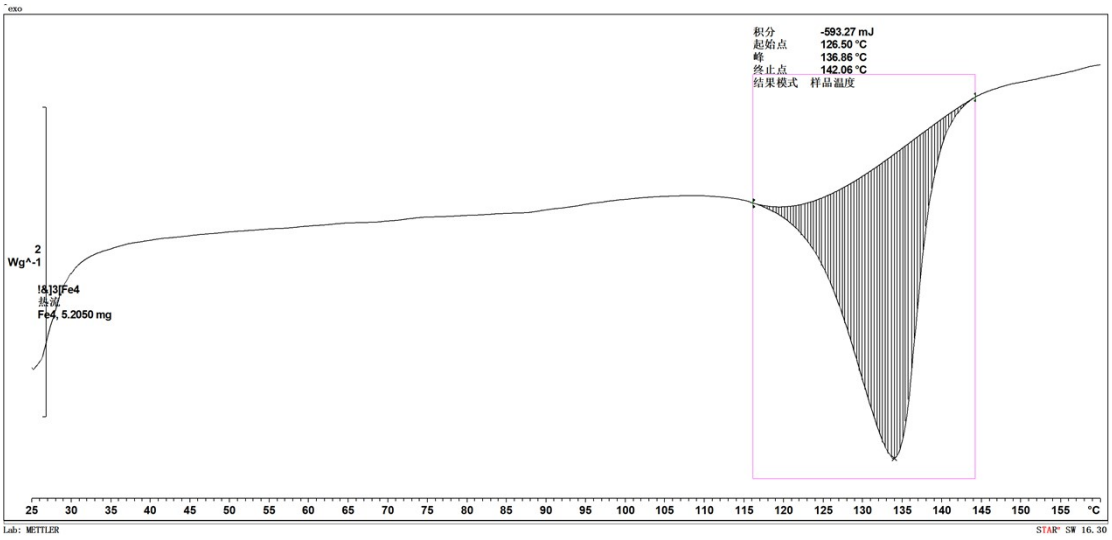


**Figure S16.** DSC thermogram of obtained polyethylene using $Fe^{Cl}$ as precatalyst and MAO as cocatalyst at 60 ℃ (Table 4, entry 2).

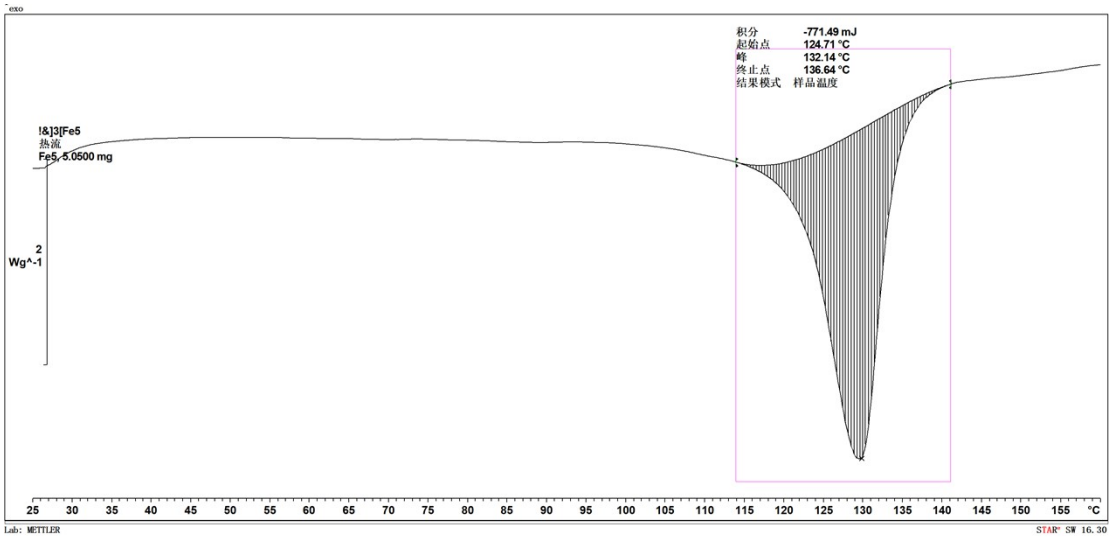


**Figure S17.** DSC thermogram of obtained polyethylene using $Fe^{F}$ as precatalyst and MAO as cocatalyst at 60 ℃ (Table 4, entry 1).

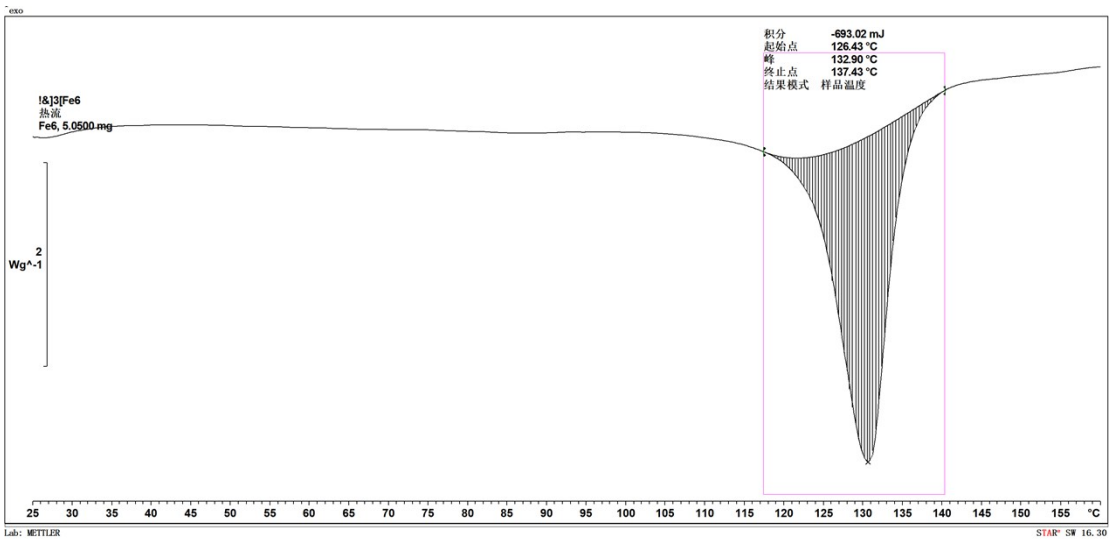


**Figure S18.** DSC thermogram of obtained polyethylene using A as precatalyst and MAO as cocatalyst at 60 ℃ (Table 4, entry 8).

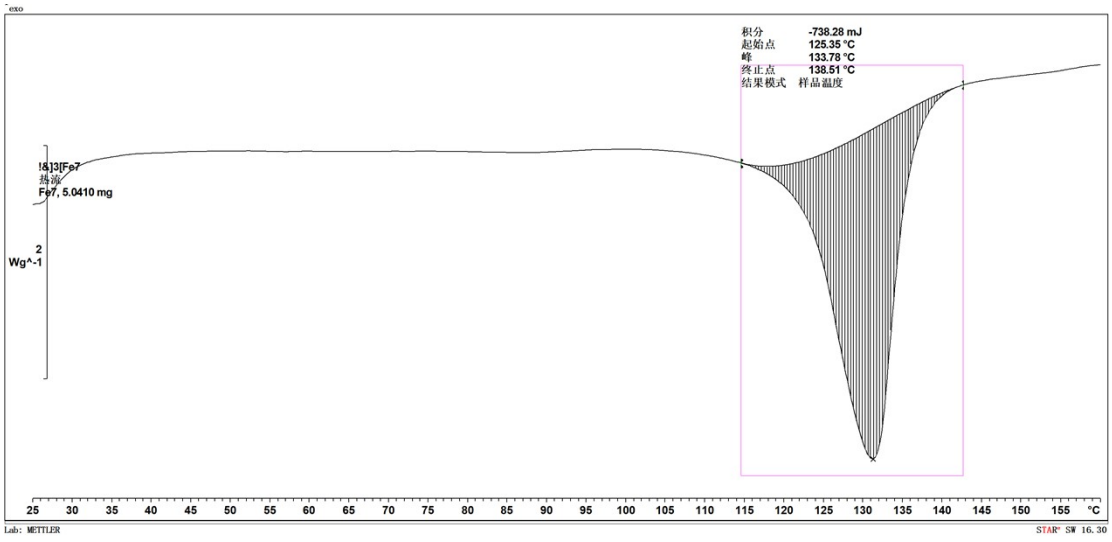


**Figure S19.** DSC thermogram of obtained polyethylene using $Fe^{iPr2}$ as precatalyst and MAO as cocatalyst at 60 ℃ (Table 4, entry 6).

## 6. $^{1}H$ and $^{13}C$ NMR of obtained polyethylene

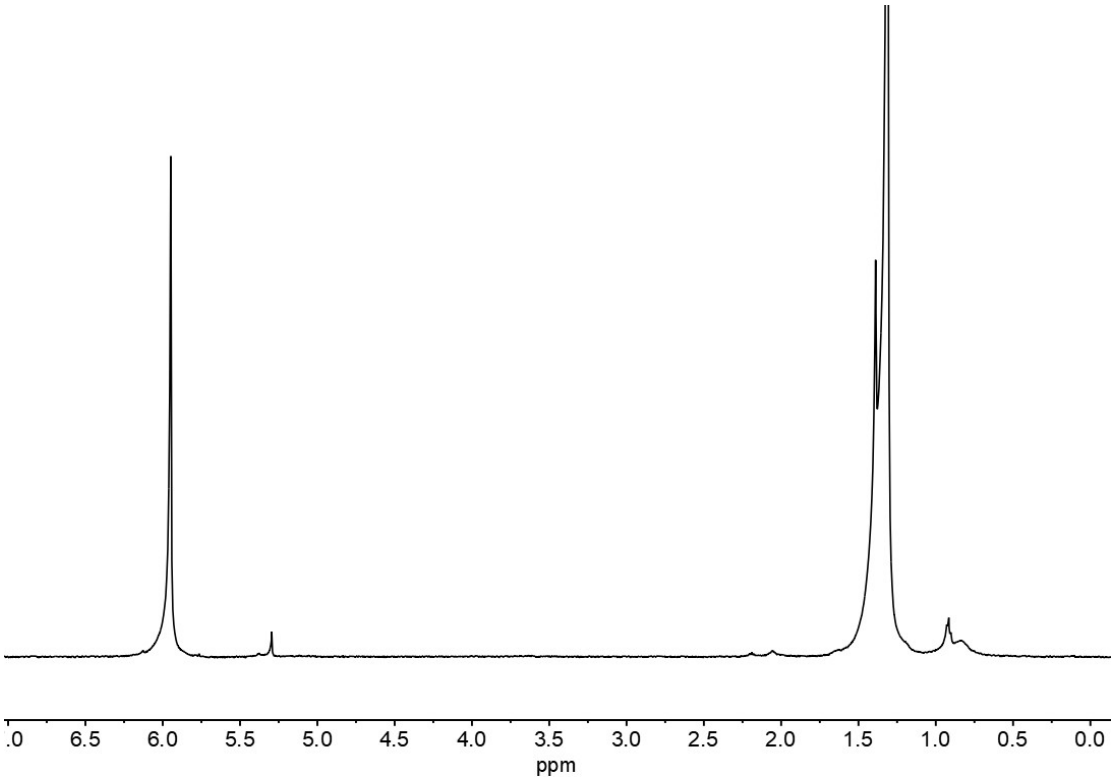


**Figure S20.** $^{1}H$ NMR spectrum of PE sample obtained by **Fe$^{Me}$**/MAO at 30 °C (Table 2, Entry 1).

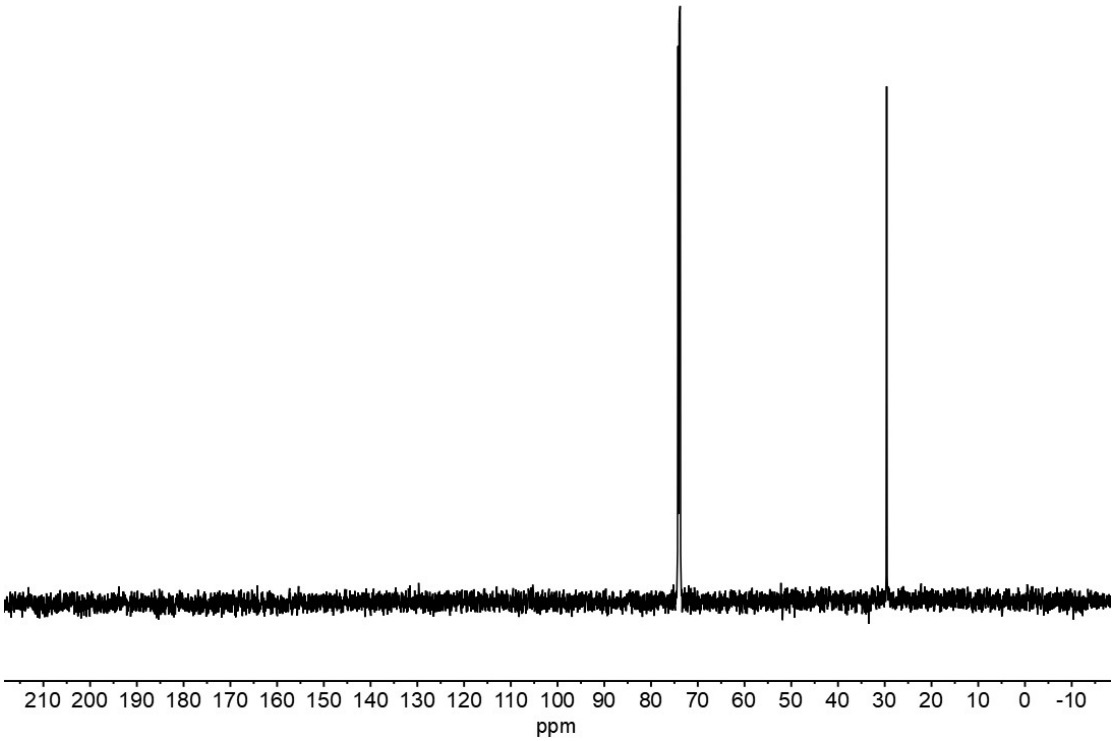


**Figure S21.** $^{13}C$ NMR spectrum of PE sample obtained by **Fe$^{Me}$**/MAO at 30 °C (Table 2, Entry 1).

## 7. References

[1] G. M. Sheldrick, SHELXTL-97, Program for the Refinement of Crystal Structures, University of Göttingen, Göttingen, Germany, 1997.